

# Boosting Automatic Exercise Evaluation Through Musculoskeletal Simulation-Based IMU Data Augmentation

Andreas Spilz<sup>1</sup>, Heiko Oppel<sup>1</sup>, and Michael Munz<sup>1,\*</sup>

<sup>1</sup>AI for Sensor Data Analytics Research Group, Ulm University of Applied Sciences, Ulm, 89081, Germany

\*michael.munz@thu.de

## ABSTRACT

Automated evaluation of movement quality holds significant potential for enhancing physiotherapeutic treatments and sports training by providing objective, real-time feedback. However, the effectiveness of deep learning models in assessing movements captured by inertial measurement units (IMUs) is often hampered by limited data availability, class imbalance, and label ambiguity. In this work, we present a novel data augmentation method that generates realistic IMU data using musculoskeletal simulations integrated with systematic modifications of movement trajectories. Crucially, our approach ensures biomechanical plausibility and allows for automatic, reliable labeling by combining inverse kinematic parameters with a knowledge-based evaluation strategy. Extensive evaluations demonstrate that augmented variants closely resembles real-world data, significantly improving the classification accuracy and generalization capability of neural network models. Additionally, we highlight the benefits of augmented data for patient-specific fine-tuning scenarios, particularly when only limited subject-specific training examples are available. Our findings underline the practicality and efficacy of this augmentation method in overcoming common challenges faced by deep learning applications in physiotherapeutic exercise evaluation.

## Introduction

Home-based training represents a vital component of many physiotherapeutic treatment strategies and has been shown to enhance patient outcomes<sup>1-4</sup>. However, these exercises are typically performed without professional oversight, presenting several challenges. The lack of supervised guidance can negatively impact adherence<sup>5</sup> to the prescribed regimen and lead to incorrect execution of the prescribed exercises<sup>6</sup>. Consequently, progress may be slowed, and in some cases, improper execution can lead to inappropriate loading or even injury. These issues can be effectively addressed by systems that monitor and analyze movements, providing real-time feedback to the user. Such systems have demonstrated the ability to improve adherence<sup>7</sup> and hold promise for enhancing the safety and efficacy of unsupervised physiotherapeutic exercises.

To address this challenge, we developed a sensor system that integrates inertial measurement units (IMUs) with deep learning algorithms to enable automated evaluation of movement patterns<sup>8</sup>. IMUs offer a portable and cost-effective means of capturing three-dimensional motion data in real time, while deep learning methods excel at identifying subtle patterns and complex relationships within large datasets. This combined approach was tested using exercises from Functional Movement Screening (FMS), a widely recognized protocol for evaluating key aspects of movement quality, including stability and mobility<sup>9,10</sup>.

A major challenge in this field is the limited availability of training data, a constraint faced by many research groups. The datasets collected by our team<sup>8</sup> and other research groups<sup>11,12</sup> exhibit three key issues: a small quantity of data points per exercise, a highly imbalanced label distribution, and a limited number of recorded subjects, leading to limited diversity in movement patterns. These data limitations impede the development of robust machine learning models for motion assessment and often lead to poor generalization, especially on unseen subjects<sup>8,13,14</sup>.

Comprehensive data collection efforts alone cannot resolve this issue. In addition to the substantial monetary and temporal resources required, it is highly challenging to recruit appropriate test participants representative of the full spectrum of movement performance. Acquiring samples of perfectly executed repetitions requires test subjects with extraordinary abilities, which are scarce within the general population. In contrast, intentionally inducing severely flawed repetitions carries an ethically unacceptable risk of injury. Given these constraints, alternative strategies have been explored to overcome the scarcity and limitations inherent in experimental data collection. Recent literature presents several promising approaches for generating artificial IMU data.

Several approaches generate IMU data based on data from other domains such as motion capture (MoCap) data<sup>15-17</sup>, video data<sup>18</sup> or pose data<sup>19</sup>. These approaches are promising, yet they only work if the corresponding MoCap, video or pose data

is available. Such data, however, is often scarce or unavailable, particularly in the context of specialized physiotherapeutic exercises.

In contrast to these methods, purely data-driven approaches use neural networks to generate synthetic data, for example by using GANs<sup>20-22</sup> or text to IMU applications such as IMU-GPT<sup>23,24</sup>. However, these models likewise depend on having enough examples in their training dataset, particularly for minority classes, to learn a valid representation. If a specific class is undersampled, these purely data-driven techniques may fail to capture its essential characteristics. Moreover, most of these approaches cannot guarantee biomechanical plausibility<sup>20-23</sup>, and none of them ensure correct class assignment for the generated samples<sup>20-24</sup>. Such limitations are especially problematic when augmenting an underrepresented class with a large volume of synthetic data: if the generated examples are biomechanically invalid or incorrectly classified, the model could learn unrealistic patterns that are not representative of real-world scenarios.

Other approaches leverage musculoskeletal models to ensure the biomechanical plausibility of generated examples. However, many of these approaches inherently preserve the original class labels (“label-preserving”). Rather than synthesizing data examples associated with different labels, their primary aim is to increase dataset variability by artificially modifying IMU sensor positioning and orientation using musculoskeletal simulations, as demonstrated by Uhlenberg et al.<sup>17</sup> and Mundt et al.<sup>16</sup>. Alternatively, Chandrasekaran et al.<sup>25</sup> increase variability by scaling the anthropometric proportions of the musculoskeletal models to represent different body morphologies. Moreover, several of these methods depend on existing MoCap data<sup>15-17</sup>, which, as previously mentioned, is often not available and very costly to obtain.

In contrast, certain approaches explicitly produce non-label-preserving data, as demonstrated by Dorschky et al.<sup>26</sup> and Renani et al.<sup>15</sup>. These approaches can generate different labels since their target parameters, for instance joint angles, can be directly extracted from the musculoskeletal simulations themselves. However, transferring these approaches to automated physiotherapeutic exercise evaluation poses a significant challenge: the relevant labels in this context cannot be directly derived from musculoskeletal simulations alone but must be inferred from multiple derived parameters, complicating the label assignment process.

Building upon the existing research, we propose a novel approach tailored to augment IMU datasets within the domain of automatic exercise evaluation, explicitly addressing the aforementioned limitations regarding data availability, biomechanical plausibility, and label assignment complexity. In summary, this paper focuses on the following key aspects:

- **Novel data augmentation method**

We introduce a novel data augmentation method to generate realistic IMU data by integrating musculoskeletal simulations with targeted modifications of movement trajectories. This approach intentionally generates examples across multiple classes while ensuring biomechanical plausibility. Notably, our method exclusively utilizes IMU data, eliminating reliance on available data from other domains.

- **Automatic labeling approach**

Our method combines inverse kinematics parameters with a knowledge-based evaluation strategy, enabling rapid and automatic derivation of accurate labels. This significantly reduces the manual effort traditionally associated with labeling physiotherapeutic exercise data.

- **Extensive evaluation of the characteristics of augmented data and their influence on the performance of a automated evaluation classifier**

We rigorously evaluate both the characteristics and practical utility of the generated data. Employing dimensionality reduction, we verify the realism and variability of the augmented dataset compared to real-world data. Additionally, controlled experiments assess how incorporating augmented data influences accuracy and generalization performance of a neural network for automatic exercise evaluation.

- **Patient-specific fine-tuning using augmented data**

We examine the effectiveness of augmented data for patient-specific fine-tuning scenarios of pretrained models. Our experiments quantify how augmented samples enhance personalized predictions, particularly in scenarios with limited subject-specific training examples.

## Methods

In this section, we first provide a detailed description of the datasets used in our study, highlighting their properties, challenges, and the respective measurement procedures. Subsequently, we outline our novel augmentation method, including preprocessing of IMU data, systematic modification of movement orientations, inverse kinematics-based validation, and the automatic labeling approach. Finally, we present our comprehensive evaluation strategy, comprising data characterization, the neural

network architecture, experimental setups assessing the utility of augmented data, and a targeted exploration of patient-specific fine-tuning scenarios.

### Used datasets

In this study, we evaluate our novel data augmentation approach using three datasets collected by our team through two separate measurement studies<sup>8,27</sup>. For more details about the measurement process and study design, please refer to the original publications. These datasets comprise three distinct exercises, each characterized by unique properties, thus posing different challenges for neural network-based evaluation methods. Specifically, we consider two FMS tasks, the Deep Squat (DS) and the Hurdle Step (HS), as well as one commonly prescribed rehabilitation exercise for patients experiencing foot drop (FDE).

### Dataset properties and challenges

The selected exercises exhibit variability in difficulty for neural network analysis based on two primary properties: class distribution and ambiguity in labeling.

The class distribution, both overall and at an individual participant level, significantly impacts dataset complexity. The Foot Drop exercise (FDE) dataset represents an optimal case with a balanced class distribution, both overall and per subject, across three categories: “correct execution” (CE), “foot drops” (FD), and “weight shift supporting leg” (WSSL). This is due to the fact that both error cases FD and WSSL were forced to happen during the exercises. Each of the seven participants contributed approximately equal repetitions across these categories, totaling around 210 repetitions<sup>27</sup> (see Figure 2 a).

The DS dataset presents a more complex scenario, characterized by an imbalanced overall class distribution and a limited representation of multiple classes per participant. With roughly 600 repetitions from 15 participants, most individuals contributed repetitions predominantly belonging to a single class (see Figure 2 b). This limited within-subject class diversity increases the challenge for neural network-based assessment.

The HS dataset represents the most complex scenario, demonstrating an even more significant imbalance in overall class distribution compared to the DS (see Figure 2 c). Similar to the DS, participants generally contributed repetitions from one or two classes, which increased the challenge for model training and evaluation.

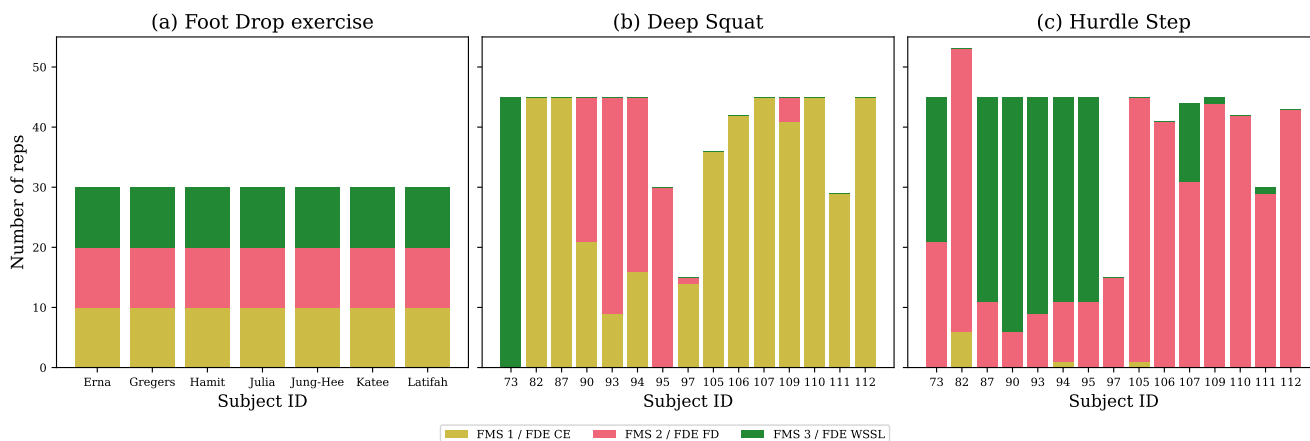


**Figure 1.** Class distribution across subjects for the, Foot Drop exercise (FDE), Deep Squat and Hurdle Step exercises. Panel (a) represents the FDE, illustrating a favorable, balanced class distribution among correct execution (CE), foot drops (FD), and weight shift supporting leg (WSSL). Panel (b) focuses on the DS, revealing a more skewed distribution overall. Most participants contributed repetitions predominantly belonging to one class, limiting within-subject diversity. This imbalance increases the classification complexity, as fewer opportunities exist to learn class distinctions within individual participants. Panel (c) displays the Hurdle Step (HS), which presents the highest degree of imbalance among the three categories. Similar to the DS, class representations tend to cluster around one or two classes per participant, intensifying the challenges for neural network analysis.

The clarity of label assignment also critically affects dataset quality. For the FDE dataset, we utilized an objective assessment methodology, classifying each repetition based on kinematic parameters derived from MoCap data. This objective labeling procedure significantly reduces ambiguity in label assignment.

In contrast, label assignment for the DS and HS exercise relied on subjective assessments by three independent physiotherapists according to predefined FMS criteria outlined by Cook et al.<sup>9,10</sup>. Each exercise repetition is rated on a scale from 1 to 3, reflecting severe movement deficiencies (1), moderate execution with minor compensations (2), or optimal execution (3).

However, due to the subjective interpretation of the FMS guidelines, substantial ambiguity arises. The percentage of ambiguous repetitions (i.e., repetitions with disagreement among raters) varies between exercises and increases complexity (see Figure 2). Specifically, the DS exhibits a notable level of ambiguity, rendering it more challenging to assess than the FDE. The HS dataset presents the highest degree of ambiguity, further complicating its evaluation. This ambiguity has previously been attributed to the inherent subjective interpretation of FMS criteria, as indicated in prior research<sup>28</sup>.

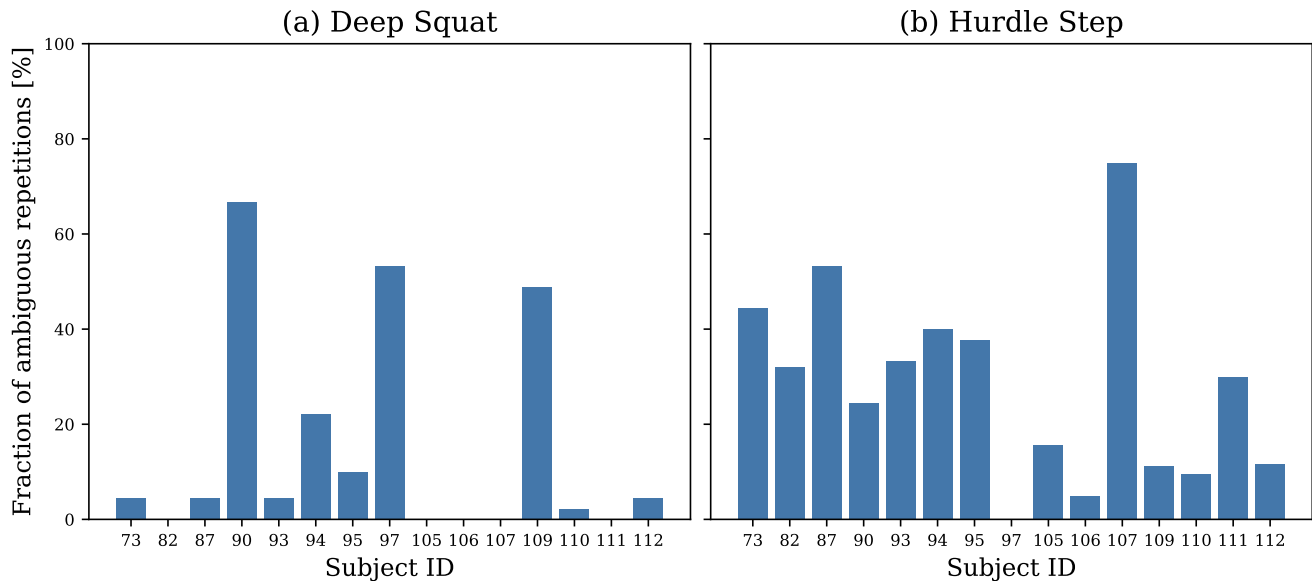


**Figure 2.** Ambiguous label assignments for the Deep Squat (DS) and Hurdle Step (HS) exercises.

Illustrated are the fractions of exercise repetitions that were deemed ambiguous (i.e., repetitions with differing ratings among independent physiotherapists) for individual participants. Panel (a) shows data for the DS exercise, while panel (b) corresponds to the HS exercise. Notably, the DS already displays a moderate extent of disagreement, whereas the HS presents the highest overall level of ambiguity. This heightened ambiguity has been linked to the inherently subjective nature of the Functional Movement Screening criteria, as described in prior work<sup>28</sup>.

In summary the presented datasets exhibit increasing complexity for neural network analysis, stemming from class imbalance and label ambiguity. The FDE dataset is the most straightforward, while the DS presents a moderate challenge, and the HS proves to be the most difficult.

### Measurement procedure

For all datasets, IMUs were strategically positioned at key anatomical locations to capture comprehensive movement data. Specifically, 15 IMUs were utilized for the FMS exercises (DS and HS), while nine IMUs were deployed for the FDE.

### Augmentation process

Our augmentation process enables the generation of modified versions of a given movement exercise based on IMU data. These variations can either represent the same movement quality label (e.g., the same FMS score) or be altered in a way that results in a different label. Since we train our neural networks on orientations rather than raw IMU data, both the input and output of our augmentation process are represented as quaternions. The following sections provide a detailed description of each step involved in the augmentation process.

### Necessary preprocessing steps

To enable the augmentation process, several preprocessing steps are required. First, the orientation of each IMU must be estimated from the raw sensor data. Depending on the dataset, different algorithms were applied. For the FMS exercises, orientation estimation was performed using the Madgwick<sup>29</sup> orientation filter (beta=0.033), which utilized accelerometer and gyroscope data to provide a stable orientation estimate<sup>8</sup>. In contrast, the foot drop rehabilitation dataset relied on the proprietary XKF3hm algorithm, which is implemented on the MVN Awinda sensors from Movella<sup>30</sup> and computes orientation directly on the device.

The estimated quaternions  $T_{IMU}$  represent the orientation of the IMU in lab space and, consequently, the orientation of the corresponding body segment to which the IMU is attached. However, due to inevitable variations in sensor placement

across different subjects, directly using these orientations would introduce inconsistencies. To address this, we define a unified coordinate system for each body segment and compute an initial transformation  $T_{offset}$  for each IMU that maps the IMU orientation to the corresponding segment coordinate system. This transformation is determined at the beginning of the recording. The segment orientation  $T_{segment}$  is then obtained using this equation:

$$T_{segment} = T_{offset} \cdot T_{IMU}$$

This standardization eliminates systematic errors caused by deviations in sensor attachment and ensures that all recorded orientations are expressed in a consistent reference frame. The exact computation method of  $T_{offset}$  is detailed in prior research<sup>8,27</sup>, whilst other methods for sensor-to-segment calibration are also applicable.

### Targeted modification of orientations

Following the preprocessing steps, the previously computed orientation trajectories  $T_{segment}$  are systematically modified to introduce variations in movement patterns. To achieve this, the quaternion-based orientation data is first converted into Euler angles. The time-dependent progression of each Euler angle of a specific segment  $s$  is defined as:

$$e_s[t] = \begin{bmatrix} \phi[t] \\ \theta[t] \\ \psi[t] \end{bmatrix},$$

corresponding to rotations around the respective axes (roll, pitch, yaw). To generate augmented motion trajectories, we modify the Euler angles using two augmentation parameters: an offset vector  $\beta$ , defining the initial posture, and a scaling vector  $\alpha$ , which adjusts the relative range of motion to match the desired target range  $\delta$ . The augmented trajectory is computed as follows:

$$e_{s,aug} = (e_s[t] - e_s[0]) \odot \alpha + \beta,$$

with

$$\alpha = \begin{bmatrix} \frac{\delta_\phi}{\max(e_\phi[t]) - \min(e_\phi[t])} \\ \frac{\delta_\theta}{\max(e_\theta[t]) - \min(e_\theta[t])} \\ \frac{\delta_\psi}{\max(e_\psi[t]) - \min(e_\psi[t])} \end{bmatrix}, \quad \beta = \begin{bmatrix} \beta_\phi \\ \beta_\theta \\ \beta_\psi \end{bmatrix}.$$

The augmentation parameters  $\beta$  and  $\delta$  are drawn from two distinct multivariate normal distributions, which are furthermore specific to a given rating, exercise, and segment.

These distributions are constructed by calculating mean and standard deviation of offsets and ranges for each Euler angle component  $c$  from available repetitions:

$$\beta_c = e_c[0], \quad \delta_c = \max(e_c[t]) - \min(e_c[t]).$$

Once these distributions have been established, they can be used to generate augmented Euler angle trajectories. If the augmentation parameters are sampled from the distributions corresponding to the original rating, the augmentation introduces moderate variations while preserving the overall movement characteristics. In contrast, selecting augmentation parameters from a distribution associated with a different rating allows for more significant modifications, enabling the generation of movement variations that reflect different execution qualities.

The parameters of these normal distributions can be established using two approaches: (1) empirical estimation from recorded datasets as shown above and (2) expert knowledge from experienced physiotherapists. Ideally, both approaches are combined: statistical patterns extracted from recorded data provide a quantitative foundation, while expert knowledge ensures that the distributions align with realistic movements. This alignment is particularly crucial in cases where the sample size for a specific class is limited. In this study, the distributions were initially generated based on available data and subsequently reviewed by experts for validation.

Figure 3 presents a visual illustration of the proposed augmentation process. It depicts the baseline and augmented Euler angle trajectories for the femur segment, along with the associated distribution parameters used to generate the augmented motions.

Following the transformation, the modified Euler angles are converted back into quaternions. Using Euler angles for augmentation offers key advantages, as they provide an intuitive representation of movement that aligns well with physiotherapeutic expertise. This interpretability is essential for validating the generated variations.

The rationale behind this approach is that variations in physiotherapeutic exercise execution are often characterized by subtle deviations in the initial posture and range of motion. By adjusting the offset parameter, variations in initial posture are introduced, while modifications to the scaling factor alter the range of motion. As a result, this method enables the generation of diverse movement instances that may either remain within the same evaluation class or represent different classes.

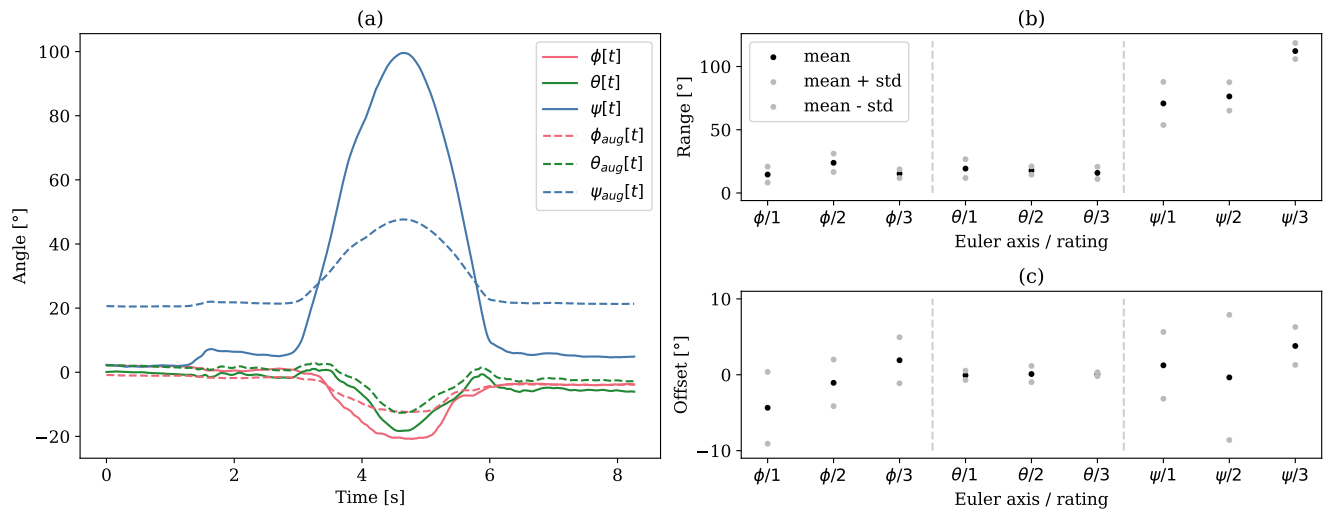


**Figure 3.** Exemplary illustration of the targeted modification of orientations using a Deep Squat (DS) repetition and the corresponding Euler angle trajectory of the right femur. (a) The original Euler angle trajectories are shown as solid lines, while the augmented trajectories are represented by dashed lines. The data was scaled and adjusted with an offset, where the augmentation parameters were sampled from the corresponding multivariate distributions. (b/c) The parameters for the range distributions (b) and offset distributions (c) for different Euler axes and rating categories are shown.

### Inverse kinematics

The transformation of the orientation data, as described above, only considers individual body segments and does not account for the kinematic dependencies between adjacent segments. To ensure that the biomechanical constraints of the human body are maintained, an inverse kinematics computation is performed based on the generated orientation trajectories and a suitable skeletal model.

For this purpose, we use the IMU Inverse Kinematics Toolbox in the open-source software OpenSim 4.5<sup>31</sup>. The skeletal model used is a customized version of the model by Rajagopal et al.<sup>32</sup> that was adapted to the specific requirements of our application. The inverse kinematics algorithm in OpenSim calculates for each time step the pose of the model that best fits the given segment orientations, while adhering to the predefined biomechanical constraints of the model.

Since the modified orientation trajectories have already been transformed into their respective segment coordinate systems in a prior step, they can be directly used to control the movement of individual segments during the computation.

The procedure ensures that the generated motion remains biomechanically plausible, respecting natural joint constraints, and thereby providing realistic augmented samples.

### Automatic labeling

The proposed augmentation technique does not inherently maintain the original class labels of the generated examples, resulting in a non-label-preserving approach. Consequently, a reliable method is necessary to determine the appropriate class for each augmented repetition. Although the distributions from which scaling factors and offsets are sampled are specific to individual classes, these distributions alone do not guarantee correct class assignments. This is because inverse kinematics computations may alter segment orientations, potentially shifting a movement into a different category. Additionally, since the augmentation parameters are drawn from probability distributions, it is possible to sample values that significantly deviate from the class-specific mean, thereby generating examples that align more closely with a different class.

One option for verifying the class labels would be to manually relabel the generated movements by expert physiotherapists using visual inspection of the reconstructed movements. However, this approach is highly time-consuming and costly. To address this challenge, we developed an automated evaluation method that classifies the generated examples based on domain knowledge about the specific exercise and kinematic information derived from the inverse kinematics computation described earlier.

This automated approach utilizes the predefined evaluation process for each FMS exercise or the definition of the error patterns in the FDE. Each exercise is characterized by multiple evaluation criteria that are either met or unmet, and an evaluation process that assigns a label based on the set of unfulfilled or fulfilled criteria (see Figure 4). Each evaluation criterion can be mapped to an evaluation parameter calculated from metrics derived from the musculoskeletal simulation, such as joint angles,

segment positions, or relative distances between anatomical points.

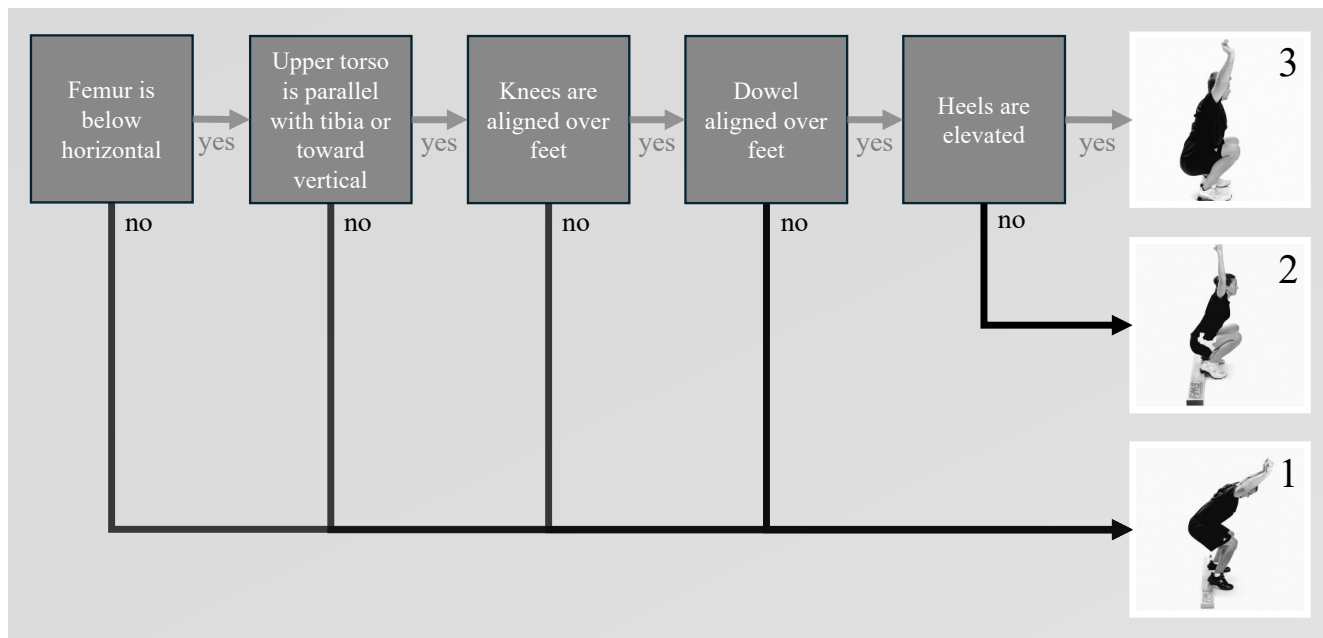


**Figure 4.** Labeling process for the Deep Squat (DS) as defined by Cook et al. Each exercise is characterized by multiple criteria (e.g., ‘Femur is below horizontal’ or ‘Heels are elevated’). Their fulfillment or violation determines the final exercise quality label.

During development, we identified challenges translating certain evaluation criteria unambiguously into specific thresholds for derived kinematic parameters. For instance, the criterion “hands above feet” used in the DS assessment lacks clarity regarding the exact anatomical reference points and acceptable deviations, leading to subjective interpretations. To resolve this ambiguity and achieve consistent labeling between real and augmented data, we developed a threshold optimization procedure based on the available real data and the original physiotherapist-assigned labels to achieve consistency between the already labeled dataset and the automatic labeling process.

To achieve this, the real data undergoes the same inverse kinematics computation as the augmented data, providing the necessary kinematic parameters for automated labeling. The real dataset is then processed through the automated classification framework, and the alignment between the automated labels and physiotherapist-assigned labels is assessed using the geometric mean across the F1-scores of the  $n$  individual classes  $GM_{F_1}$ :

$$GM_{F_1} = \left( \prod_{i=1}^n F_{1,i} \right)^{\frac{1}{n}}.$$

To optimize the threshold values, we employ a random search strategy, a commonly used approach in hyperparameter tuning. During optimization, the underlying ruleset remains unchanged, but thresholds are uniformly sampled from ranges defined by the observed minimum and maximum parameter values in the real data. We evaluated a total of 10 million threshold combinations per exercise, selecting the set yielding the highest  $GM_{F_1}$  score for subsequent classification of augmented data. The achieved  $GM_{F_1}$  scores for the three used exercises are denoted in table 1. This procedure ensures that the classification framework aligns as closely as possible with expert-based assessment, enabling reliable labeling of the augmented repetitions.

| Exercise   | Deep Squat | Hurdle Step | Foot Drop exercise |
|------------|------------|-------------|--------------------|
| $GM_{F_1}$ | 0.839      | 0.754       | 0.958              |

**Table 1.** Best achieved geometric mean of F1-Scores  $GM_{F_1}$  using the described random search methodology for the three used datasets.

## Evaluation

This section describes the experiments conducted to characterize the augmented repetitions and investigate their impact on training a neural network.

### **Generation of augmented examples**

For each dataset, augmented examples were generated based on the recorded repetitions. Specifically, from each real repetition, an equal number of examples were generated for each of the three possible classes, resulting in approximately 20,000 generated examples per dataset. The computation time required to generate one example corresponded roughly to the execution duration of the respective movement. This computational performance was determined on a desktop computer equipped with an AMD Ryzen 5 3600X 6-Core Processor operating at 3.79 GHz. To ensure only unambiguous examples were created, a preliminary selection process was implemented. Only examples whose automatic labeling matched the class assigned by the selected distribution were retained for further analysis.

### **Characteristics comparison**

To gain an initial understanding of the characteristics of the augmented examples, we conducted a dimensionality reduction using the t-distributed Stochastic Neighbor Embedding (t-SNE) method. This analysis was performed separately for each dataset, involving both the real data and a subset of 1200 augmented examples. To ensure a balanced representation, the augmented examples were selected such that an equal number of examples per class were included for each subject.

The t-SNE analysis was carried out using the implementation provided by scikit-learn (version 1.5.2). While most parameters were set to their default values, the perplexity parameter was specifically adjusted to 15. Prior to the final analysis, parameter variation was conducted within a sensible range to confirm that the observed characteristics were consistently detectable across different parameter configurations.

### **Neural network architecture and training details**

For our evaluation, we implemented a neural network based on a convolutional neural network (CNN) architecture to assess the effect of augmented data on model performance. The network architecture initially includes a convolutional layer consisting of 16 filters with a kernel size of  $5 \times 5$ , designed to capture local spatial features within the input data. Subsequently, a dropout layer with a rate of 0.2 is applied to mitigate overfitting.

Following the convolutional stage, the extracted features are flattened and processed by fully connected layers. The first dense layer comprises 512 neurons and is followed by another dropout layer (rate 0.2). A second dense layer with 128 neurons, again followed by a dropout layer (rate 0.2), further refines the feature representation. Finally, an output layer consisting of 3 neurons is used to perform the classification task.

All layers except the output layer use the Rectified Linear Unit (ReLU) as their activation function, while the output layer utilizes a softmax activation function to convert the neural network's output into probabilities corresponding for each respective class.

The convolutional layer and both dense layers include L2 regularization with a factor of  $10^{-3}$ . All layers are initialized using the Glorot Uniform method to ensure efficient convergence during training.

For optimization, we employed the Adam optimizer with a learning rate of  $10^{-4}$ . Training was conducted with mini-batches of size 32. Additionally, to further enhance training efficiency and reduce overfitting, an early stopping strategy was implemented, terminating training if no improvement in the validation loss was observed for 10 consecutive epochs. Final model evaluation was performed using the model weights that achieved the highest macro F1-score on the validation set.

### **Dataset preprocessing**

The data samples undergo the following preprocessing steps to be compatible with the neural network. The quaternion-based orientation sequences of the individual body segments are linearly interpolated to a standardized temporal length of 256 time steps, employing the Spherical Linear Interpolation technique (SLERP)<sup>33</sup>. Subsequently, the interpolated orientation trajectories for each IMU are arranged in a row-wise format, constructing an input representation suitable for CNN processing. This arrangement enables the neural network to effectively leverage the inherent temporal and spatial dependencies present in the IMU orientation data.

### **Experiments**

To assess the properties of the augmented repetitions and their impact on classification performance, we conducted a series of experiments. The analysis consisted of two main parts:

First, we investigated how the augmented repetitions compare to real repetitions in terms of their characteristics and variance. To address this, we defined three experimental scenarios:

- Training on real data, testing on real data (TRTR): This scenario served as a baseline to establish performance benchmarks.

- Training on augmented data, testing on real data (TATR): This scenario assessed the extent to which augmented data could capture the variance of real-world data.
- Training on real data, testing on augmented Data (TRTA): Conversely, this setup examined if the variance present in the augmented data was sufficiently represented by real training data.

To ensure robust and reliable results, the described scenarios were evaluated using a 5-fold cross-validation approach. The 5-fold cross-validation was carefully designed to ensure that each subset consistently contained examples from all subjects and a comparable proportion of examples for each class, thereby ensuring representative results.

In each iteration, four folds of the dataset were used for training, with 80% of this training set employed for model training and the remaining 20% for validation. The remaining fold was held out and used exclusively for testing. To ensure balanced class distributions in training and validation datasets, oversampling was applied where necessary. In scenarios involving augmented data, we consistently used 1200 examples for training, and 240 examples each for validation and testing. These augmented examples were selected uniformly across all classes and subjects, ensuring a representative dataset composition. Importantly, each augmented example was generated exclusively from the real data examples within the respective dataset partition, preventing information leakage between dataset splits.

Second, we analyzed the influence of the combination of real and augmented samples on the classification performance. These scenarios were analyzed using a leave-one-subject-out cross validation (LOSOCV) approach. This method was chosen explicitly because it effectively simulates the realistic scenario where the model must generalize across individuals with distinct movement characteristics. In each LOSOCV iteration, one subject was entirely excluded from the training and validation sets and included solely in the test set. The remaining subjects' data were divided into training (80%) and validation (20%) subsets. Real data in these sets were oversampled when necessary to ensure a balanced class distribution between real samples. Additionally 1,200 augmented examples were added to the training set and 240 to the validation set, again ensuring balanced class distribution per subject. Depending on the number of subjects, this resulted in a 15-fold LOSOCV for the DS and HS datasets and a 7-fold LOSOCV for the FDE dataset. Specifically we investigated these two scenarios:

- Training on real data, testing on real data using LOSOCV (TRTR-LOSO): This scenario served as a baseline to establish performance benchmarks.
- Training on real and augmented Data, testing on real data using LOSOCV (TRATR-LOSO): This scenario assessed the influence of augmented data on performance on an unseen subject.

### ***Patient specific finetuning***

Typically, the available datasets contain a limited number of participants, providing insufficient data to train neural networks capable of fully capturing the variety of movements found in the general population. Consequently, the concept of patient-specific fine-tuning appears beneficial for enhancing network performance on individual cases.

In this context, we investigate the impact of fine-tuning within a realistic scenario. Specifically, we assume that for a previously unseen subject, only two movement examples belonging to a single class are available. This assumption aligns with a realistic clinical scenario, as it is common at the beginning of treatment to have only a few recorded executions of a movement, typically representing a consistent performance level.

To systematically analyze the impact of data augmentation within this fine-tuning scenario, we conducted two distinct experiments:

For the first experiment, we investigated the influence of patient-specific fine-tuning without using augmented data. The initial model was trained solely on the original dataset, excluding data from the new subject. During fine-tuning, we used the two available real repetitions from the new subject, supplemented by two real examples per relevant movement class from the original dataset (TRTR-FT).

The second experiment used additional augmented data. The starting point was a network trained initially without data from the new subject but including augmented training data. During the fine-tuning step, we used the two real repetitions from the new subject and further augmented these examples. Specifically, eight augmented examples per missing movement class and six augmented examples for the already recorded class were generated (TRATR-FT).

In both experiments, we applied a slanted triangular learning rate schedule [QUELLE], peaking at a learning rate of  $10^{-4}$  after five epochs and continuing training for a total of 20 epochs. Fine-tuning was limited to the dense layers of the model, while the CNN-based feature extraction layers remained fixed, as preliminary analyses suggested that these layers sufficiently generalize across subjects and do not require further adaptation. Fine-tuning was performed only for those subjects who had not already achieved a macro-F1 score of 1.0.

## Results

This section summarizes the experimental results. We first characterize the distribution of real and augmented samples in a t-SNE plot. We then assess the impact of augmented data on classification performance across different evaluation scenarios, followed by an analysis of subject-specific effects. Finally, we evaluate the benefits of incorporating augmented data into patient-specific fine-tuning strategies.

### Characteristics of real and augmented samples

Figure 5 exemplarily presents the results of dimensionality reduction using t-SNE for both FDE and HS samples. The results for the DS samples are not visualized but resemble the observations for the HS samples.

In the FDE dataset, augmented examples closely cluster around the corresponding real examples, suggesting that the augmentation process replicates the real-world movement characteristics. Additionally, the embedded space reveals no clear separation between different classes. Notably a prominent subject-specific clustering pattern is observed, with augmented examples consistently positioned within these clusters.

The HS dataset exhibits a more diverse distribution pattern. Here, multiple clusters contain predominantly or exclusively real or augmented data points. However, no distinct separation between the classes is observable here either. Notably, a clear distinction between the subjects is still maintained.

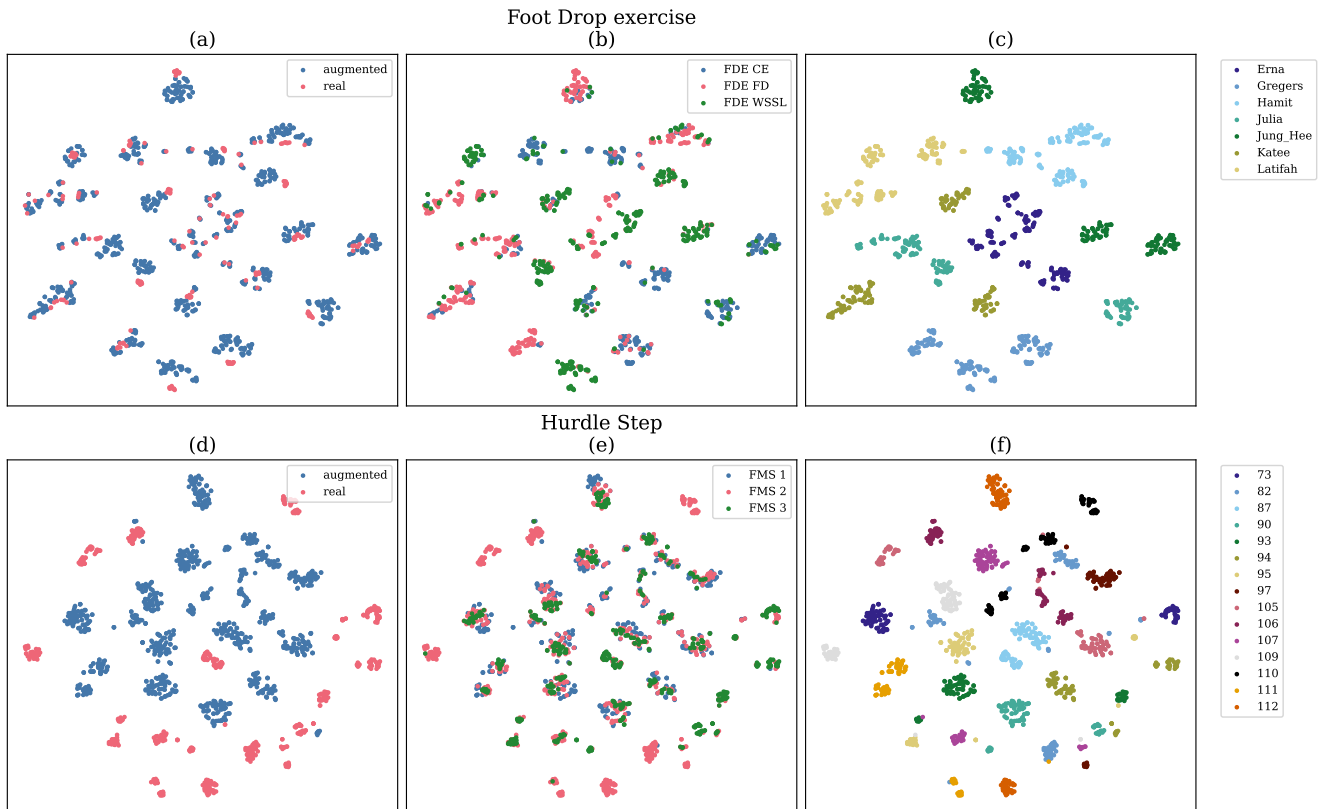


**Figure 5.** Exemplary visualization of the t-SNE-based dimensionality reduction for augmented and real data in the Foot Drop exercise (FDE) and Hurdle Step (HS) datasets.

For the FDE dataset (a–c), augmented samples consistently cluster among their real counterparts, reflecting realistic replication of movement characteristics. The low-dimensional space shows strong subject-specific clustering without distinct class separation. In the HS dataset (d–f), several clusters contain predominantly real or augmented instances. Nonetheless, no clear class segregation is apparent, while subject-specific grouping remains clearly discernible. Although not depicted here, the DS data exhibit a similar distributional behavior to that of the HS samples.

### Influence on classification performance

Table 2 provides a summary of the overall and class-specific classification performance across three distinct training and testing scenarios using a 5-fold cross-validation for the FDE, DS and HS datasets.

Training on real data and testing on real data, the FDE (0.95) and DS (0.92) datasets yielded high mean macro F1-scores, while the HS dataset reached a slightly lower value of 0.79. A closer inspection of the class-wise F1-scores reveals that the model trained on FDE performs consistently well across all classes. For DS, class 3 was classified most accurately, followed by class 2, while performance for class 1 was comparatively lower. In contrast, the model trained on HS shows good classification results for classes 2 and 3, but a substantial drop in performance for class 1, highlighting this class as a primary source of misclassification within this dataset.

In the TATR scenario, the FDE dataset achieved a mean macro F1 score of 0.93 nearly identical to that achieved with TRTR. However, the DS dataset performance decreased noticeably, with the mean macro F1-score dropping to 0.81. While class 3 continued to be classified perfectly, performance for class 1 declined slightly, and the F1-score for class 2 dropped significantly to 0.60. The most substantial performance degradation was observed on the HS dataset, where the mean macro F1-score fell to 0.51. All class-wise F1-scores decreased: class 2 remained the most robust with a score of 0.79, whereas class 3 dropped to 0.63 and class 1 performed very poorly, achieving only 0.11.

When models were trained on real data and evaluated on augmented test samples (TRTA), a clear drop in performance was observed across all datasets. For FDE, the mean macro F1-score decreased to 0.63. Class-wise F1-scores indicate that all three classes experience comparable issues, with macro F1-scores ranging from 0.58 to 0.70. The DS dataset exhibited a more pronounced decline, with a mean macro F1-score of only 0.46. All three classes showed similarly poor results, with F1-scores ranging from 0.37 to 0.51. The HS dataset suffered the most substantial degradation, reaching a macro F1-score of just 0.29. While class 3 and class 2 still achieved scores of 0.51 and 0.34 respectively, the model completely failed to detect class 1, yielding a F1-score of 0.00.

| Exercise           | Configuration | Macro F1             | F1 Score 1           | F1 Score 2           | F1 Score 3           |
|--------------------|---------------|----------------------|----------------------|----------------------|----------------------|
| Foot Drop exercise | TRTR          | <b>0.952 ± 0.03</b>  | <b>0.943 ± 0.049</b> | <b>0.955 ± 0.044</b> | 0.959 ± 0.031        |
|                    | TATR          | 0.933 ± 0.032        | 0.913 ± 0.065        | 0.921 ± 0.027        | <b>0.965 ± 0.031</b> |
|                    | TRTA          | 0.634 ± 0.055        | 0.62 ± 0.062         | 0.697 ± 0.053        | 0.584 ± 0.064        |
| Deep Squat         | TRTR          | <b>0.923 ± 0.007</b> | <b>0.945 ± 0.009</b> | <b>0.823 ± 0.013</b> | <b>1.0 ± 0.0</b>     |
|                    | TATR          | 0.814 ± 0.033        | 0.842 ± 0.046        | 0.601 ± 0.056        | 1.0 ± 0.0            |
|                    | TRTA          | 0.455 ± 0.035        | 0.507 ± 0.052        | 0.373 ± 0.113        | 0.483 ± 0.055        |
| Hurdle Step        | TRTR          | <b>0.792 ± 0.127</b> | <b>0.627 ± 0.336</b> | <b>0.902 ± 0.023</b> | <b>0.849 ± 0.033</b> |
|                    | TATR          | 0.513 ± 0.087        | 0.113 ± 0.157        | 0.795 ± 0.037        | 0.631 ± 0.095        |
|                    | TRTA          | 0.285 ± 0.017        | 0.0 ± 0.0            | 0.342 ± 0.031        | 0.513 ± 0.036        |

**Table 2.** Summary of the overall and class-specific performance across three training–testing configurations for the Foot Drop exercise (FDE), Deep Squat (DS), and Hurdle Step (HS) datasets.

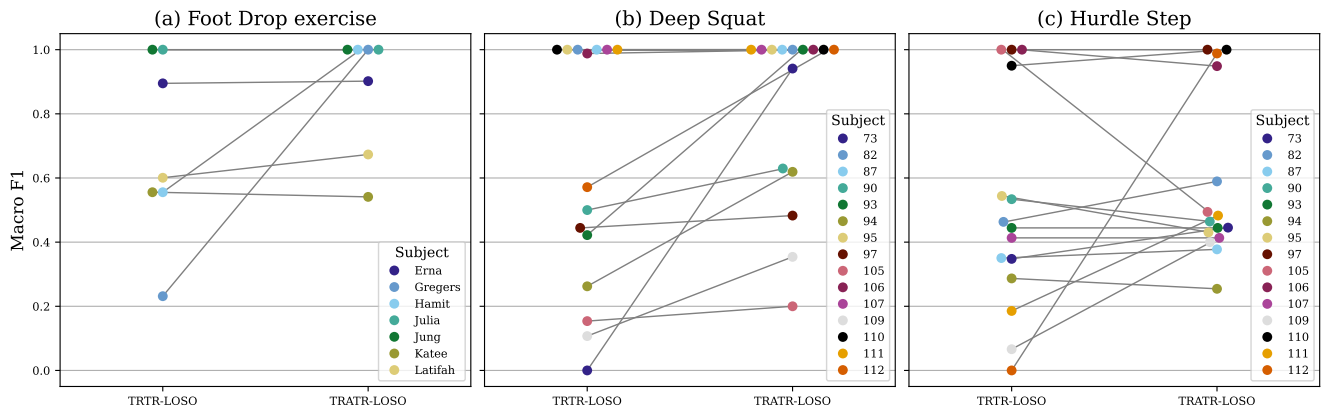
The reported results include the mean and standard deviation of the achieved Macro- $F_1$  score, as well as the mean and standard deviation of each class-specific  $F_1$  score, derived from a 5-fold cross-validation procedure. Compared are three different scenarios: training on real data and testing on real data (TRTR), training on augmented data and testing on real data (TATR) and training on real data and testing on augmented data (TRTA).

Figure 6 compares the subject-wise performance on real data between a classifier trained on exclusively real data (TRTR-LOSO) and a classifier trained on real and augmented data (TRATR-LOSO).

For the FDE dataset, subjects who already achieved high macro F1-scores with real-only training retained their strong performance when augmented data were included. Notably, subjects Hamit and Gregers, who performed poorly without augmentation, reached perfect classification performance when trained with additional augmented data. For other subjects, the improvement was only marginal.

In the DS dataset, the use of augmented data led to a consistent and substantial increase in classification performance across nearly all subjects. Particularly, subjects 73, 93, and 112 exhibited exceptional gains, transitioning from macro F1-scores below 0.6 to values exceeding 0.94. Importantly, subjects who were already well-classified under the real-only condition maintained their high performance.

Results for the HS dataset were more heterogeneous. While most subjects experienced minor improvements or degradations, subject 112 demonstrated a substantial performance increase. Conversely, subject 105 showed a notable decline. Overall, the majority of subjects remained in the 0.2–0.6 performance range across both training conditions. However, with augmented training, no subject achieved a macro F1-score below 0.2, whereas under real-only training, subjects 109, 111, and 112 fell below this threshold.



**Figure 6.** Comparison of subject-wise performance (LOSO) on real data between a classifier trained on exclusively real data (TRTR-LOSO) and a classifier trained on a combination of real and augmented data (TRATR-LOSO). This evaluation is performed for three datasets: Foot Drop exercise (panel a), Deep Squat (panel b) and Hurdle Step (panel c)

### Patient specific finetuning

To evaluate the subject-specific impact of fine-tuning, we compared classification performance before and after applying a fine-tuning step. This analysis was performed separately for models trained without and with augmented samples. For each of the three datasets, models were first trained in a LOSOCV setting and subsequently fine-tuned using a subset of real data or a combination of real and augmented data from the left-out subject. The corresponding macro F1-scores on the remaining test data of the same subject are summarized in Figure 7.

For the FDE dataset, fine-tuning without augmentation led to moderate performance gains for most subjects. A particularly notable improvement was observed for subject Gregers, whose macro F1-score increased from 0.21 to 0.79. In contrast, subject Erna experienced a slight decline, dropping from 0.88 to 0.8. When augmented data were used during training, the initial performance levels were already considerably higher, resulting in overall smaller changes through fine-tuning. However, in this setting, all subjects benefitted from fine-tuning, ultimately achieving near-perfect macro F1-scores above 0.92.

In the DS dataset, fine-tuning without augmentation substantially improved performance for nearly all subjects, with the exception of subject 90, who exhibited a slight decrease. Subjects 105 and 112 reached perfect performance levels through fine-tuning, while others remained within the 0.46–0.51 range. When augmented data were used, the baseline performance was already consistently higher across subjects. Fine-tuning yielded a pronounced benefit for subject 105, while for the remaining subjects, it resulted in only minor increases or decreases. All but subjects 90, 94, 97, and 105 achieved near-perfect classification performance post fine-tuning, whereas the latter group remained in the range of 0.48 to 0.61.

The HS dataset presented the most heterogeneous results. Without augmentation, fine-tuning had mixed effects: while subject 112 showed an exceptional improvement, most other subjects fluctuated between modest gains and drops, with final performance values clustering between 0.31 and 0.49. When augmented data were included, the initial performance levels were slightly elevated, but the effects of fine-tuning were generally limited. In this setting, changes in performance were small.

### Discussion

In this work, we introduced a novel approach for data augmentation in IMU based exercise evaluation, specifically tailored for physiotherapeutic exercises. In the following we want to discuss our main contributions and future implications.

The t-SNE dimensionality reduction analysis offered valuable visualizations that highlighted the similarities between the real and augmented data samples. Interestingly, the FDE dataset exhibited clusters containing both real and augmented examples, suggesting that the fundamental properties of the exercise repetitions were preserved. Conversely, the visualization of the HS dataset shows a more distinct separation between real and augmented examples, with fewer mixed clusters observed. However, this observation does not necessarily imply substantial discrepancies between the augmented and real data. Rather, it may indicate that the augmented HS samples encompass a broader range of movement variations compared to the real data, which may itself exhibit only limited variability in execution.

The frequent occurrence of clusters encompassing examples from multiple classes highlights the complexity involved in class separation within the dataset. This complexity underscores the need for classification methods capable of capturing nuanced and intricate differences between classes. Employing neural networks, as applied in this study, is therefore justified due to their ability to effectively model such complex decision boundaries.

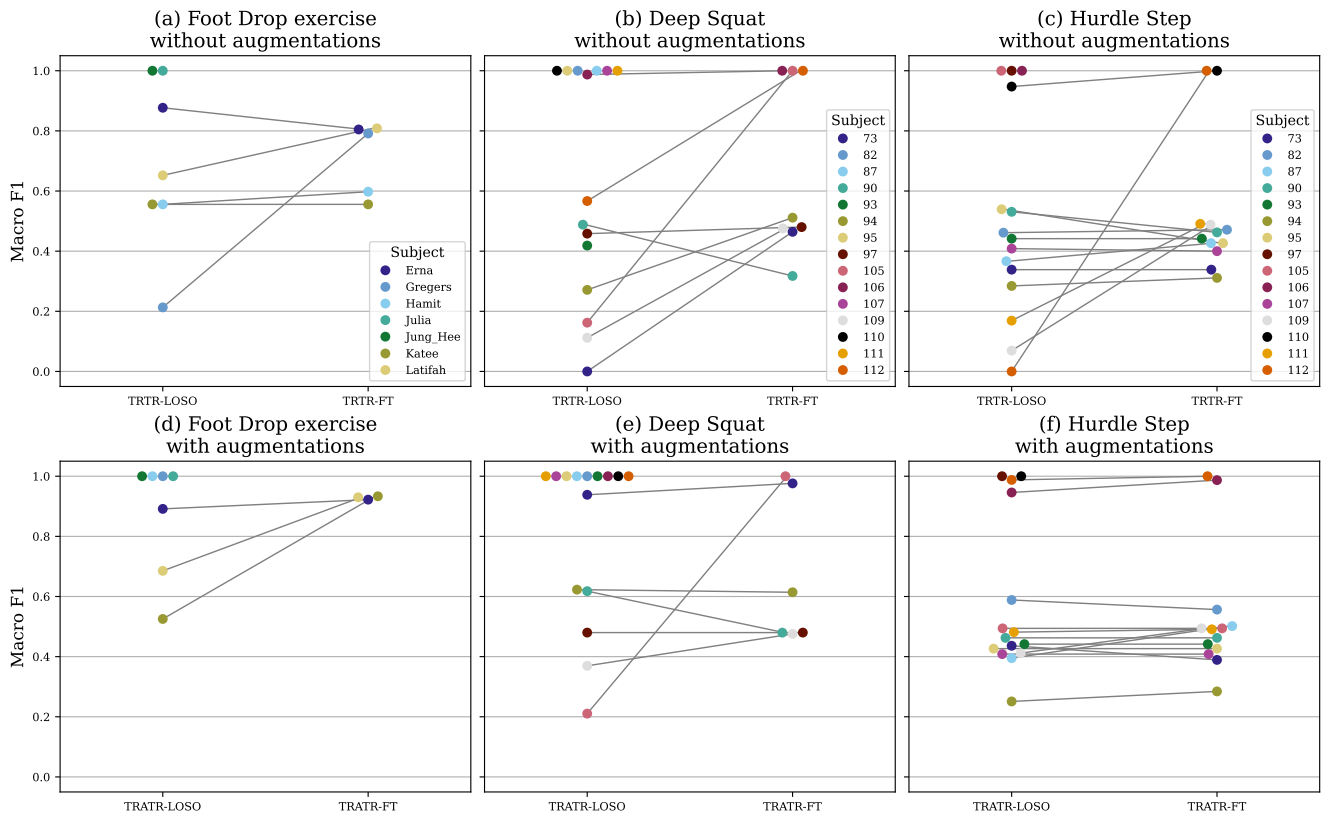


**Figure 7.** Comparison of subject-wise patient-specific finetuning performance with and without augmented data. The comparison takes place between a baseline trained without augmented data (TRTR-LOSO) which is finetuned using only real data (TRTR-FT) and a baseline trained on real and augmented data (TRATR-LOSO) which is finetuned using real and augmented data (TRATR-FT). This evaluation is performed for three datasets: Foot Drop exercise (panel a and d), Deep Squat (panel b and e) and Hurdle Step (panel c and f).

Moreover, the formation of subject-specific clusters underscores the substantial impact of individual movement characteristics on the movement data. The observation that both real and augmented examples form these clusters indicates that the presented augmentation method generates samples which preserve patient-specific characteristics. Such augmented data holds particular value for approaches like patient-specific finetuning, as it could increase the amount and variability within the very limited available training data.

Overall, the insights gained from the t-SNE analysis validate the chosen data augmentation approach, demonstrating its effectiveness in preserving movement characteristics while enhancing dataset diversity.

Comparison of the results of the TATR with the TRTR scenario for the FDE exercise reveals that the classification performance remains essentially unchanged when exclusively augmented data is used for training. This result strongly indicates that the augmented data accurately captures the essential movement characteristics of the FDE exercise, and covers at least the same variance range as the real data.

In contrast, the findings for the DS and HS datasets present a divergent pattern. The classification performance decline is noticeable (from 0.92 to 0.81 for DS and from 0.79 to 0.51 for HS) when training relies solely on augmented data. Specifically, class-level analyses for DS indicate particular challenges in accurately replicating real examples of class 2 within the augmented dataset. Similarly, for the HS exercise, discrepancies appear pronounced, especially in classes 1 and 3. A plausible explanation for the observed discrepancies is possibly the different frequencies with which certain movement patterns occur in the real and augmented data set. Due to the relatively small number of available real samples, particularly notable in the HS exercise with only eight instances for class 1, there is a possibility that the augmented examples reflect motion patterns that, although valid, are not adequately represented in the few available real examples. Consequently, this divergence could contribute to misclassifications. Additionally, the substantial proportion of ambiguously evaluated repetitions within the real DS and HS datasets could further intensify these misclassification issues as there are no corresponding examples in the augmented dataset. Additionally, the TRTA scenario reveals that training solely on real data consistently yields poor performance when evaluated

on augmented data across all exercises. Based on the findings from the TRTA and the TATR scenario, we hypothesize that the augmented data encompasses a broader range of variance and characteristics compared to the real data, and therefore could serve as a valuable addition to the training dataset.

Collectively, the evidence supports the conclusion that improved training outcomes are likely achieved by combining real and augmented data, thereby ensuring coverage of a broad variance range.

The results obtained from our LOSOCV experiments demonstrate that incorporating augmented data can enhance the performance of exercise evaluation models. It is important to notice, that the extent of this improvement is subject-dependent. Depending on the participant, the utilization of augmented data contributed to a noticeable, and in some cases, substantial increase in performance. However, there were also a limited number of subjects where performance either remained relatively unchanged or slightly declined. We hypothesize that the additional use of augmented data may lead to subtly altered decision boundaries, which in turn could slightly degrade performance for these specific participants. A single subject (105) exhibited a pronounced degradation in performance upon integration of augmented data. This phenomenon warrants further investigation and will be discussed comprehensively in a later section of this work.

We hypothesize that the lack of performance improvement observed for certain individuals in the LOSOCV scenario can be attributed to the absence of their unique movement patterns in the training data. Although our augmentation approach increases the variability within the training dataset, it preserves the participant-specific characteristics of the original baseline repetitions, as confirmed by our methodological rationale and the t-SNE analysis. Consequently, despite the enhanced diversity introduced through augmentation, the participant-specific motion patterns of the left-out subject may not be represented in the training set, thus limiting the potential performance gains derived from the augmented repetitions.

This consideration further implies that methods such as participant-specific fine-tuning could potentially lead to substantial classification improvements, particularly for those subjects who do not benefit sufficiently from general augmentation strategies.

We analyzed the influence of augmented repetitions on the fine-tuning process through the comparison of the results of the TRTR-FT and TRATR-FT experiments. Results from experiments on the FDE dataset clearly demonstrate that fine-tuning enables participant-specific movement patterns to be effectively learned from just two real examples of a single class, provided that these examples are supplemented with augmented data derived from the same two examples but representing additional classes. This result further supports the hypothesis that the proposed augmentation approach preserves participant-specific movement patterns, which constitutes a clear advantage in the described scenario.

Nevertheless, a substantial number of participants in the DS and HS datasets did not exhibit significant performance gains from fine-tuning, with or without augmented data. We hypothesize that this can be primarily attributed to ambiguity in the associated class labels. This issue is clearly illustrated in the DS dataset, where participants 90, 94, 97, and 109 consistently perform at low accuracy levels despite fine-tuning. Upon examining Figure 8, it is evident that these test subjects have a distinct higher proportion of ambiguous repetitions (20 - 70% of the test subjects' repetitions) compared to the other test subjects in the DS data set. Although fine-tuning allows the decision boundary to be effectively adapted to an individual subject, the substantial proportion of ambiguous repetitions in this test set leads to many repetitions appearing virtually identical, yet being assigned different labels. Consequently, the adjusted decision boundary produces the effect illustrated in Figure 8: While the classification performance improves for one class, it simultaneously deteriorates for the other, resulting in a macro F1-score that remains approximately unchanged.

A similar pattern emerges in the HS dataset, where the general proportion of ambiguous repetitions is substantially higher than in the DS dataset. Apart from subjects 97, 105, 106, 109, 110, and 112, ambiguous repetition proportions consistently exceed 20%, resulting in poor performance. Correspondingly, subjects 110, 106, 112, and 97 achieve strong performance even before fine-tuning. Conversely, subjects 105 and 109 still perform poorly despite a low proportion of ambiguous repetitions. For these subjects, performance issues likely stem from their class distribution. Subject 105 has a single example of class 1, a class represented by only eight examples across the entire dataset and therefore very little variance, defined by ambiguous rating criteria ("loses balance"), which consequently impairs the macro F1-score (see Figure 8 and Figure 7). Similarly, subject 109 includes a single ambiguous example from class 3, adversely affecting their overall macro F1-score.

We hypothesize that this high proportion of ambiguous repetitions in some participants likewise influences the TRATR-LOSO outcomes. As previously noted, some participants showed a slight or even marked decline in performance when augmented data were introduced (particularly subject 105). Because the labeling of the augmented examples is significantly clearer than that of the real data, it may shift the decision boundary in a way that no longer aligns with the real, ambiguous data. Consequently, the model's ability to recognize these participants' real examples can deteriorate, especially when substantial portions of their dataset are affected by ambiguous labeling.

Our data augmentation approach successfully generates biomechanically valid examples, capable of representing both identical and distinct movement classes. This capability is particularly beneficial for addressing imbalanced datasets, as it enables the targeted generation of rare or specific movement patterns that are typically underrepresented. Importantly, the method is not inherently restricted to the presented exercises; rather, it can be extended to additional exercises, provided that at

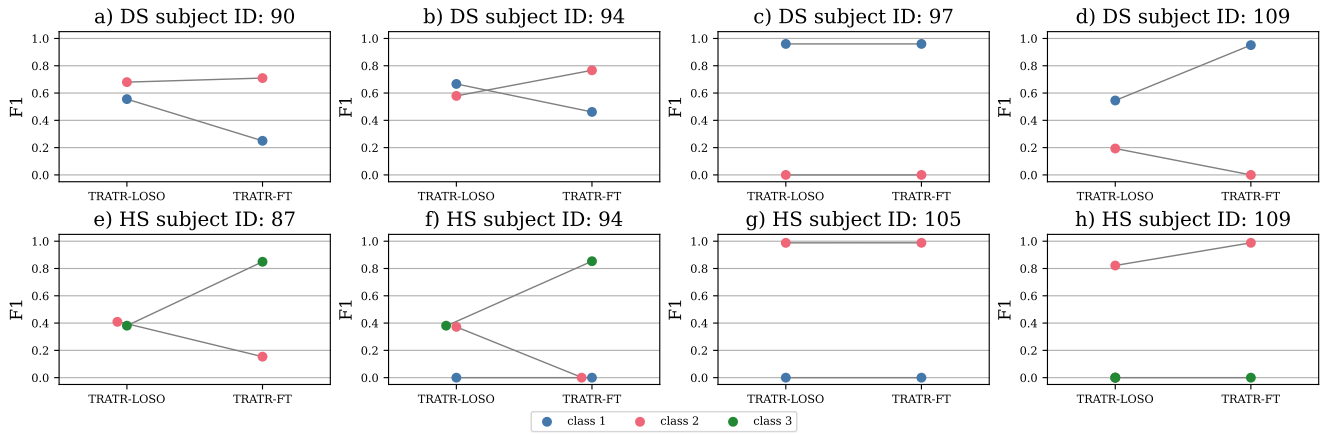


**Figure 8.** Comparison of subject-wise performance between the baseline and the finetuned model. The comparison takes place between a baseline trained on real and augmented data (TRATR-LOSO) which is finetuned using real and augmented data (TRATR-FT). This evaluation is performed exemplarily for four subjects of the Deep Squat (DS) dataset (panel a - d) and for four subjects of the Hurdle Step (HS) dataset (panel e - h).

least a minimal number of real repetitions are recorded using a suitable IMU setup and sufficient domain knowledge regarding correct execution and variations is available. In physiotherapeutic contexts, such requirements are commonly met, making this approach particularly suitable for clinical applications.

However, extending this method to new exercises does require adjustments. Specifically, the automatic labeling must be adapted to reflect new evaluation criteria, necessitating the definition of new decision thresholds and distributions for each Euler angle, derived either from real data, domain knowledge, or a combination thereof.

The computational demands of our augmentation process remain comparatively low. Unlike approaches based on generative Neural Networks like GANs, our approach does not require substantial GPU resources; indeed, the computational time needed for generating an augmented example approximately equals the duration of the original exercise, a highly acceptable cost for practical applications.

One limitation of the procedure presented is the lack of subject-specific scaling of the biomechanical model. This was omitted because the required anthropometric data for the DS and HS data set are not available. Introducing individual scaling could potentially result in more personalized augmented examples, although it remains unclear whether this increased subject specificity would positively or negatively impact the overall generalization of neural network models. Furthermore, the biomechanical model used currently offers limited degrees of freedom in the torso region and therefore represents a simplified approximation of human anatomy. Thus, for exercises predominantly involving torso movements, a more detailed biomechanical representation of this region would be advisable to enhance the realism of generated examples.

The automatic labeling approach ensures that the generated examples reliably belong to a specific class. For this purpose, predefined evaluation criteria are systematically analyzed on the basis of information from the inverse kinematics. The use of clearly defined decision limits in this automated process guarantees consistent and reproducible labeling of the generated examples.

As presented earlier, the performance of the automated labeling approach, when compared to the labels assigned by physiotherapists, demonstrated satisfactory results for its intended application. Specifically, the FDE dataset achieved a geometric macro-F1 score of 0.958, indicating highly accurate classification. However, the DS and HS datasets yielded somewhat lower scores of 0.839 and 0.75, respectively, suggesting more challenges in effectively automating the labeling process for these exercises. This performance decrease can be attributed to two primary factors. Firstly, both the DS and HS datasets contain a considerable proportion of repetitions that were ambiguously evaluated by the physiotherapists, leading to inevitable misclassifications, as rigid automated thresholds are unable to replicate the subjective fluctuations of human evaluators. Secondly, some assessment criteria (e.g. “loses balance”) are inherently ambiguously defined, making it challenging to translate them into evaluation rules that can be automatically assessed. Consequently, there are discrepancies between the automatic and human evaluation. This issue should be considered when adapting the approach to additional exercises. In collaboration with domain experts, the definition of the evaluation criteria should be refined to ensure they can be clearly translated into evaluation rules.

However, it is crucial to emphasize that the automated labeling system should not be viewed as a replacement for neural network-based classification. A key limitation is the extensive data requirements of the automated labeling, which relies on inverse kinematics calculations to determine joint angles, positions, and related metrics. These calculations necessitate at

least one IMU per moving segment, making it impossible to reduce the number of sensors for complex exercises. Currently, our neural network based classification also employs a high number of IMUs. However, ongoing research within our group specifically investigates methods to reduce the required number of IMUs for neural network-based classification, aiming to enhance practical applicability in clinical settings.

In this study, we evaluated a novel IMU data augmentation method using three distinct datasets representing varying levels of complexity, primarily driven by differences in class balance and label ambiguity. We demonstrated that our proposed augmentation approach can improve classification performance by addressing class imbalance and increasing variability within the training dataset, especially in combination with strategies such as subject-specific fine-tuning. Particularly notable improvements were achieved on the FDE dataset, which benefits from clearly defined and objective labels. However, datasets characterized by higher levels of subjective label ambiguity (DS and HS) revealed inherent limitations of augmentation alone. Thus, addressing label ambiguity emerges as a critical requirement for further progress. Future research should prioritize developing specialized methods to systematically manage ambiguity, enabling neural networks to consistently deliver accurate and meaningful evaluations and thereby improve the practical utility of automated physiotherapeutic feedback systems.

## Data available

The datasets generated during and/or analyzed during the current study are available from the corresponding author on reasonable request.

## References

1. Ashari, A., Hamid, T. A., Hussain, M. R. & Hill, K. D. Effectiveness of Individualized Home-Based Exercise on Turning and Balance Performance Among Adults Older than 50 yrs. *Am. J. Phys. Medicine & Rehabil.* **95**, 355–365, DOI: [10.1097/phm.0000000000000388](https://doi.org/10.1097/phm.0000000000000388) (2016).
2. Latham, N. K. *et al.* Effect of a Home-Based Exercise Program on Functional Recovery Following Rehabilitation After Hip Fracture: A Randomized Clinical Trial. *JAMA* **311**, 700–708, DOI: [10.1001/jama.2014.469](https://doi.org/10.1001/jama.2014.469) (2014).
3. Gelaw, A. Y., Janakiraman, B., Gebremeskel, B. F. & Ravichandran, H. Effectiveness of Home-based rehabilitation in improving physical function of persons with Stroke and other physical disability: A systematic review of randomized controlled trials. *J. Stroke Cerebrovasc. Dis. The Off. J. Natl. Stroke Assoc.* **29**, 104800, DOI: [10.1016/j.jstrokecerebrovasdis.2020.104800](https://doi.org/10.1016/j.jstrokecerebrovasdis.2020.104800) (2020).
4. Flynn, A., Allen, N. E., Dennis, S., Canning, C. G. & Preston, E. Home-based prescribed exercise improves balance-related activities in people with Parkinson’s disease and has benefits similar to centre-based exercise: a systematic review. *J. Physiother.* **65**, 189–199, DOI: [10.1016/j.jphys.2019.08.003](https://doi.org/10.1016/j.jphys.2019.08.003) (2019).
5. Argent, R., Daly, A. & Caulfield, B. Patient Involvement With Home-Based Exercise Programs: Can Connected Health Interventions Influence Adherence? *JMIR mHealth uHealth* **6**, e47, DOI: [10.2196/mhealth.8518](https://doi.org/10.2196/mhealth.8518) (2018).
6. Faber, M. *et al.* The majority are not performing home-exercises correctly two weeks after their initial instruction—an assessor-blinded study. *PeerJ* **3**, e1102, DOI: [10.7717/peerj.1102](https://doi.org/10.7717/peerj.1102) (2015).
7. Lang, S., McLelland, C., MacDonald, D. & Hamilton, D. F. Do digital interventions increase adherence to home exercise rehabilitation? A systematic review of randomised controlled trials. *Arch. Physiother.* **12**, 24, DOI: [10.1186/s40945-022-00148-z](https://doi.org/10.1186/s40945-022-00148-z) (2022).
8. Spilz, A. & Munz, M. Automatic Assessment of Functional Movement Screening Exercises with Deep Learning Architectures. *Sensors* **23**, 5, DOI: [10.3390/s23010005](https://doi.org/10.3390/s23010005) (2023). Number: 1 Publisher: Multidisciplinary Digital Publishing Institute.
9. Cook, G., Burton, L., Hoogenboom, B. J. & Voight, M. Functional movement screening: the use of fundamental movements as an assessment of function - part 1. *Int. journal sports physical therapy* **9**, 396–409 (2014).
10. Cook, G., Burton, L., Hoogenboom, B. J. & Voight, M. Functional movement screening: the use of fundamental movements as an assessment of function-part 2. *Int. journal sports physical therapy* **9**, 549–63 (2014).
11. Xing, Q.-J. *et al.* Functional movement screen dataset collected with two Azure Kinect depth sensors. *Sci. Data* **9**, 104, DOI: [10.1038/s41597-022-01188-7](https://doi.org/10.1038/s41597-022-01188-7) (2022).
12. Wu, W.-L., Lee, M.-H., Hsu, H.-T., Ho, W.-H. & Liang, J.-M. Development of an Automatic Functional Movement Screening System with Inertial Measurement Unit Sensors. *Appl. Sci.* **11**, 96, DOI: [10.3390/app11010096](https://doi.org/10.3390/app11010096) (2020).

13. Scheurer, S., Tedesco, S., O'Flynn, B. & Brown, K. N. Comparing Person-Specific and Independent Models on Subject-Dependent and Independent Human Activity Recognition Performance. *Sensors* **20**, 3647, DOI: [10.3390/s20133647](https://doi.org/10.3390/s20133647) (2020).
14. Kianifar, R., Lee, A., Raina, S. & Kulic, D. Automated Assessment of Dynamic Knee Valgus and Risk of Knee Injury During the Single Leg Squat. *IEEE journal translational engineering health medicine* **5**, 2100213, DOI: [10.1109/JTEHM.2017.2736559](https://doi.org/10.1109/JTEHM.2017.2736559) (2017).
15. Sharifi Renani, M., Eustace, A. M., Myers, C. A. & Clary, C. W. The Use of Synthetic IMU Signals in the Training of Deep Learning Models Significantly Improves the Accuracy of Joint Kinematic Predictions. *Sensors* **21**, 5876, DOI: [10.3390/s21175876](https://doi.org/10.3390/s21175876) (2021).
16. Mundt, M. *et al.* Estimation of Gait Mechanics Based on Simulated and Measured IMU Data Using an Artificial Neural Network. *Front. Bioeng. Biotechnol.* **8**, DOI: [10.3389/fbioe.2020.00041](https://doi.org/10.3389/fbioe.2020.00041) (2020).
17. Uhlenberg, L., Ole Haeusler, L. & Amft, O. SynHAR: Augmenting Human Activity Recognition With Synthetic Inertial Sensor Data Generated From Human Surface Models. *IEEE Access* **12**, 194839–194858, DOI: [10.1109/ACCESS.2024.3513477](https://doi.org/10.1109/ACCESS.2024.3513477) (2024).
18. Kwon, H. *et al.* IMUTube: Automatic Extraction of Virtual on-body Accelerometry from Video for Human Activity Recognition. *Proc. ACM Interact. Mob. Wearable Ubiquitous Technol.* **4**, 87:1–87:29, DOI: [10.1145/3411841](https://doi.org/10.1145/3411841) (2020).
19. Zolfaghari, P. *et al.* Sensor Data Augmentation from Skeleton Pose Sequences for Improving Human Activity Recognition. In *2024 International Conference on Activity and Behavior Computing (ABC)*, 1–8, DOI: [10.1109/ABC61795.2024.10652200](https://doi.org/10.1109/ABC61795.2024.10652200) (2024).
20. Norgaard, S., Saeedi, R., Sasani, K. & Gebremedhin, A. H. Synthetic Sensor Data Generation for Health Applications: A Supervised Deep Learning Approach. In *2018 40th Annual International Conference of the IEEE Engineering in Medicine and Biology Society (EMBC)*, 1164–1167, DOI: [10.1109/EMBC.2018.8512470](https://doi.org/10.1109/EMBC.2018.8512470) (2018).
21. Mohammadzadeh, M., Ghadami, A., Taheri, A. & Behzadipour, S. cGAN-based high dimensional IMU sensor data generation for enhanced human activity recognition in therapeutic activities. *Biomed. Signal Process. Control.* **103**, 107476, DOI: [10.1016/j.bspc.2024.107476](https://doi.org/10.1016/j.bspc.2024.107476) (2025).
22. Zhao, J., Obonyo, E. & Yin, Q. Improving posture recognition among construction workers through data augmentation with generative adversarial network. *IOP Conf. Series: Earth Environ. Sci.* **1101**, 092005, DOI: [10.1088/1755-1315/1101/9/092005](https://doi.org/10.1088/1755-1315/1101/9/092005) (2022).
23. Leng, Z., Kwon, H. & Ploetz, T. Generating Virtual On-body Accelerometer Data from Virtual Textual Descriptions for Human Activity Recognition. In *Proceedings of the 2023 ACM International Symposium on Wearable Computers, ISWC '23*, 39–43, DOI: [10.1145/3594738.3611361](https://doi.org/10.1145/3594738.3611361) (Association for Computing Machinery, New York, NY, USA, 2023).
24. Leng, Z. *et al.* IMUGPT 2.0: Language-Based Cross Modality Transfer for Sensor-Based Human Activity Recognition. *Proc. ACM on Interactive, Mobile, Wearable Ubiquitous Technol.* **8**, 1–32, DOI: [10.1145/3678545](https://doi.org/10.1145/3678545) (2024).
25. Chandrasekaran, M., Francik, J. & Makris, D. Gait Data Augmentation using Physics-Based Biomechanical Simulation, DOI: [10.48550/arXiv.2307.08092](https://doi.org/10.48550/arXiv.2307.08092) (2023). ArXiv:2307.08092 [cs].
26. Dorschky, E. *et al.* CNN-Based Estimation of Sagittal Plane Walking and Running Biomechanics From Measured and Simulated Inertial Sensor Data. *Front. Bioeng. Biotechnol.* **8**, DOI: [10.3389/fbioe.2020.00604](https://doi.org/10.3389/fbioe.2020.00604) (2020).
27. Oppel & Spilz. Orthokidataset. *tbd* (2025).
28. Shultz, R., Anderson, S. C., Matheson, G. O., Marcello, B. & Besier, T. Test-Retest and Interrater Reliability of the Functional Movement Screen. *J. Athl. Train.* **48**, 331–336, DOI: [10.4085/1062-6050-48.2.11](https://doi.org/10.4085/1062-6050-48.2.11) (2013).
29. Madgwick, S. O. H., Harrison, A. J. L. & Vaidyanathan, R. Estimation of IMU and MARG orientation using a gradient descent algorithm. In *2011 IEEE International Conference on Rehabilitation Robotics*, 1–7, DOI: [10.1109/ICORR.2011.5975346](https://doi.org/10.1109/ICORR.2011.5975346) (2011).
30. Paulich, M., Schepers, M., Rudigkeit, N. & Bellusci, G. Xsens MTw Awinda: Miniature Wireless Inertial-Magnetic Motion Tracker for Highly Accurate 3D Kinematic Applications. Tech. Rep., XSENS Technologies B.V. (2018).
31. Delp, S. L. *et al.* OpenSim: open-source software to create and analyze dynamic simulations of movement. *IEEE transactions on bio-medical engineering* **54**, 1940–1950, DOI: [10.1109/TBME.2007.901024](https://doi.org/10.1109/TBME.2007.901024) (2007).
32. Rajagopal, A. *et al.* Full-Body Musculoskeletal Model for Muscle-Driven Simulation of Human Gait. *IEEE Transactions on Biomed. Eng.* **63**, 2068–2079, DOI: [10.1109/tbme.2016.2586891](https://doi.org/10.1109/tbme.2016.2586891) (2016).

33. Shoemake, K. Animating rotation with quaternion curves. *SIGGRAPH Comput. Graph.* **19**, 245–254, DOI: [10.1145/325165.325242](https://doi.org/10.1145/325165.325242) (1985).

### **Author contributions statement**

A.A. contributed to conceptualization, methodology, data analysis, AI model development, carried out the experiments, analyzed the results and wrote the first draft. H.O. contributed conceptualization, analyzed the results and contributed to subsequent drafts. M.M. contributed conceptualization, analyzed the results, supervised the project and contributed to subsequent drafts. All authors reviewed the manuscript.

### **Competing interests**

The authors declare no competing interests